Annual Review of Earth and Planetary Sciences

Atlantic-Pacific Asymmetry in Deep Water Formation

David Ferreira,[1] Paola Cessi,[2] Helen K. Coxall,[3] Agatha de Boer,[3] Henk A. Dijkstra,[4] Sybren S. Drijfhout,[5] Tor Eldevik,[6,7] Nili Harnik,[8] Jerry F. McManus,[9] David P. Marshall,[10] Johan Nilsson,[11] Fabien Roquet,[11] Tapio Schneider,[12] and Robert C. Wills[13]

[1]Department of Meteorology, University of Reading, Reading RG6 6BB, United Kingdom; email: d.g.ferreira@reading.ac.uk

[2]Scripps Institution of Oceanography, University of California, San Diego, La Jolla, California 92093, USA

[3]Bolin Centre for Climate Research and Department of Geological Sciences, Stockholm University, 10691 Stockholm, Sweden

[4]Institute for Marine and Atmospheric Research Utrecht, Department of Physics and Astronomy, Utrecht University, 3584 CC Utrecht, The Netherlands

[5]Ocean and Earth Science, National Oceanography Centre Southampton, University of Southampton, Southampton SO14 3ZH, United Kingdom

[6]Geophysical Institute, University of Bergen, 5020 Bergen, Norway

[7]Bjerknes Centre for Climate Research, 5020 Bergen, Norway

[8]Department of Geophysics, Tel Aviv University, 69978 Tel Aviv, Israel

[9]Lamont-Doherty Earth Observatory, Columbia University, Palisades, New York 10964, USA

[10]Department of Physics, University of Oxford, Oxford OX1 3PU, United Kingdom

[11]Department of Meteorology, Stockholm University, 10691 Stockholm, Sweden

[12]California Institute of Technology, Pasadena, California 91125, USA

[13]Department of Atmospheric Sciences, University of Washington, Seattle, Washington 98195, USA

Annu. Rev. Earth Planet. Sci. 2018. 46:327–52

First published as a Review in Advance on March 15, 2018

The *Annual Review of Earth and Planetary Sciences* is online at earth.annualreviews.org

https://doi.org/10.1146/annurev-earth-082517-010045

Keywords

meridional overturning circulation, salinity, hydrological cycle, multiple equilibria, climate, deep water formation

Abstract

While the Atlantic Ocean is ventilated by high-latitude deep water formation and exhibits a pole-to-pole overturning circulation, the Pacific Ocean does

not. This asymmetric global overturning pattern has persisted for the past 2–3 million years, with evidence for different ventilation modes in the deeper past. In the current climate, the Atlantic-Pacific asymmetry occurs because the Atlantic is more saline, enabling deep convection. To what extent the salinity contrast between the two basins is dominated by atmospheric processes (larger net evaporation over the Atlantic) or oceanic processes (salinity transport into the Atlantic) remains an outstanding question. Numerical simulations have provided support for both mechanisms; observations of the present climate support a strong role for atmospheric processes as well as some modulation by oceanic processes. A major avenue for future work is the quantification of the various processes at play to identify which mechanisms are primary in different climate states.

1. INTRODUCTION

In the modern climate system, deep waters are formed in the North Atlantic, but not in the North Pacific. In the Labrador Sea and Nordic Seas, deep water forms during winter when heat loss to the atmosphere destabilizes the water column, resulting in intense convection that can extend down to 2,000 m depth (Marshall & Schott 1999, Weaver et al. 1999). Nothing similar is observed in the North Pacific, where convection occurs only near continents and does not reach deep into the ocean.

The Atlantic basin is characterized by a deep meridional overturning circulation (MOC) of hemispheric scale (**Figure 1*a***), associated with the export of dense cold water to the Southern Ocean and the compensating flow of upper warm and salty water toward high latitudes, referred to as the Atlantic meridional overturning circulation (AMOC) (see Wunsch & Heimbach 2013 for a review). The actual overturning of the AMOC takes place through the gradual densification and consequent sinking of the cyclonic boundary currents of the Nordic and Labrador Seas as they give up heat to the atmosphere and the convective interior (e.g., Straneo 2006). An analogous Pacific meridional overturning circulation (PMOC) is absent in the Pacific (**Figure 1*a***). The Pacific Ocean is mainly ventilated from the south, while its upper circulation is dominated by shallow wind-driven cells. This asymmetry in ventilation is evident in the estimated mean age of water masses, which measures the elapsed time since their last exposure to the atmosphere (**Figure 1*b***).

The Atlantic-Pacific asymmetry shapes climate differences between the two basins. Most notably, the northward AMOC heat transport accounts for about 60% of the 1.2 PW peak Atlantic transport near 20°N (Talley 2003, Ferrari & Ferreira 2011). This AMOC heat transport warms the Northern Hemisphere by about 1°C relative to the Southern Hemisphere, with larger regional effects (partly due to sea-ice feedbacks) of up to 6–8°C in the Nordic Seas, Scandinavia, and Western Europe (e.g., Vellinga & Wood 2002; see also **Figure 2*b***).

The focus of this review is the following question: Why is there an AMOC but not a PMOC? Numerous explanations can be found in the literature, but a consensus has yet to emerge. It is a puzzling state of affairs: The AMOC and its variability (natural and anthropogenically forced) generate considerable interest (Buckley & Marshall 2016), but we do not have clear explanations for its existence or for the absence of a PMOC.

The fact that there is substantial formation of deep water at all, in the Atlantic and/or the Pacific, is remarkable. For deep convection to occur, deep waters must, at least occasionally, be more buoyant than the dense water formed at the surface. Because oceans are differentially forced at the surface, mechanical forcing is needed to push buoyant fluid down (Sandström 1916, Kuhlbrodt et al. 2007). This is primarily done by the wind stress in the Southern Ocean circumpolar region, where buoyancy surfaces are mechanically steepened at much greater depths than in basins

MOC: meridional overturning circulation

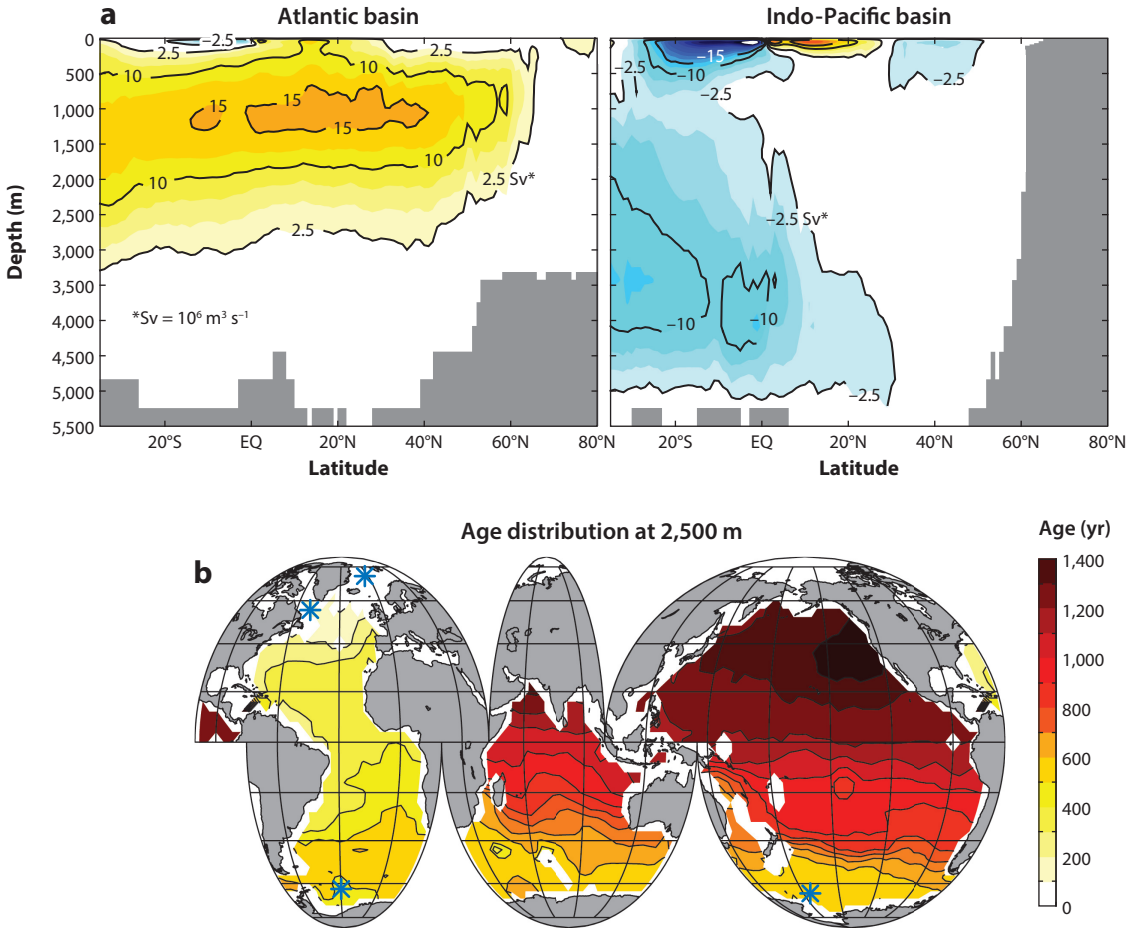

Figure 1

(*a*) Meridional overturning circulation [in Sverdrups (Sv)] (from the ECCOv4 ocean reanalysis; Forget et al. 2015) for the Atlantic basin (*left*) and for the Indo-Pacific basin (*right*). Red/blue shading denotes clockwise/counterclockwise circulations. (*b*) The mean age of water masses at 2,500 m depth; main convection sites are indicated with blue stars (data set from Gebbie & Huybers 2012).

with meridional boundaries, and by tidal and wind-generated internal waves that break and mix buoyancy downward in the ocean interior (Gnanadesikan 1999, Wolfe & Cessi 2010, Nikurashin & Vallis 2012). However, this perspective, including recent studies that consider two differentiated northern basins (Talley 2013, Thompson et al. 2016), does not address the causes of the Atlantic-Pacific asymmetry.

The preferential sinking of deep water in the North Atlantic appears fundamentally linked to the higher salinity of the basin (**Figure 2*a***) (Warren 1983). Deep convection is density driven and depends on heat loss as well as on the salinity of the surface waters. Proposals to explain the asymmetry in surface salinity broadly fall into two families. The salinity contrast can be driven from the surface by differences in net precipitation (precipitation minus evaporation) (H1), or it can result from differences in oceanic circulations and salt transport (H2). In the H1 limit, atmospheric processes are the drivers, while the ocean takes a relatively passive role. In the H2 limit, two possibilities arise: Circulation differences are caused by asymmetries in basin geometry,

Net precipitation ($P - E$): precipitation minus evaporation

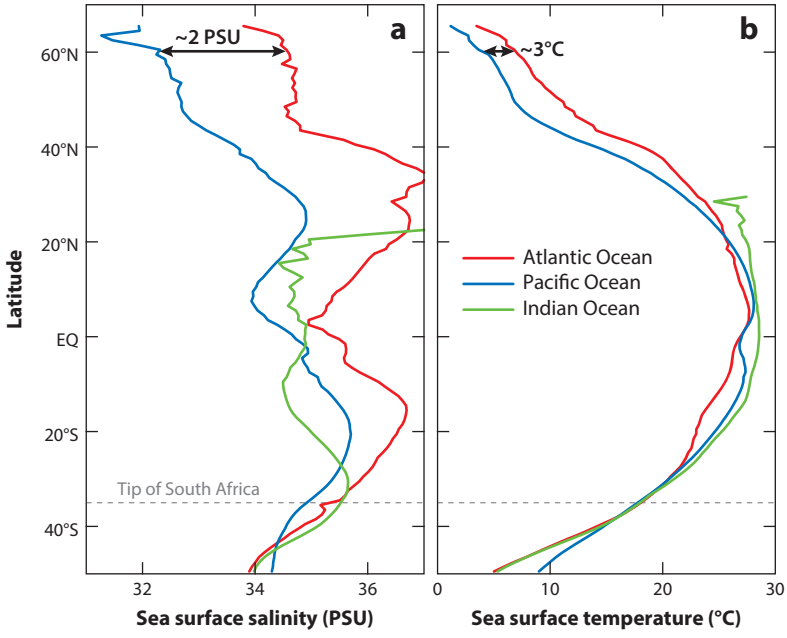

Figure 2

Observed (*a*) sea surface salinity and (*b*) sea surface temperature averaged over the period 1955–2012 and zonally from the *World Ocean Atlas 2013* (Zweng et al. 2013) for the Atlantic, Pacific, and Indian Oceans.

leading to differences in oceanic salinity and temperature advection that favor sinking in the Atlantic (H2a), or the AMOC itself is the cause of the asymmetries between the basins, importing the salt that makes the Atlantic basin saltier (H2b). This positive salt-advection feedback would create a preferred state with sinking in the Atlantic. However, with a weakened AMOC, it would further weaken the circulation, resulting in a collapsed AMOC (Stommel 1961, Rooth 1982). H2b allows multiple states of the MOC, and it could also act in the Pacific; H1 and H2a assign a greater role to basin geometry and may imply uniqueness of the AMOC.

We begin this review by putting the AMOC/PMOC problem in the context of past climates to show how the current asymmetry has evolved (Section 2). Section 3 covers atmospheric mechanisms (H1). Sections 4 and 5 discuss oceanic mechanisms (H2). Section 4 describes local determinants of the asymmetry, such as geometrical factors that tend to align with H2a. Section 5 focuses on mechanisms relying on a more active role for the oceans and exchanges of salt between the Atlantic and other oceans. Finally, Section 6 proposes avenues to move toward a more comprehensive understanding of the Atlantic-Pacific asymmetry.

2. THE ATLANTIC AND PACIFIC MERIDIONAL OVERTURNING CIRCULATION IN THE PAST

Deciphering the development of the deep ocean circulation is a broad area of active research that encompasses proxy development, deep ocean drilling programs, laboratory analysis, and modeling efforts. Both the proxies and the models have large uncertainties, but a common picture can be attempted by considering all the available evidence together. While a comprehensive review is not possible here, we present a tentative overview of the evolution of global deep water formation and overturning (**Figure 3**).

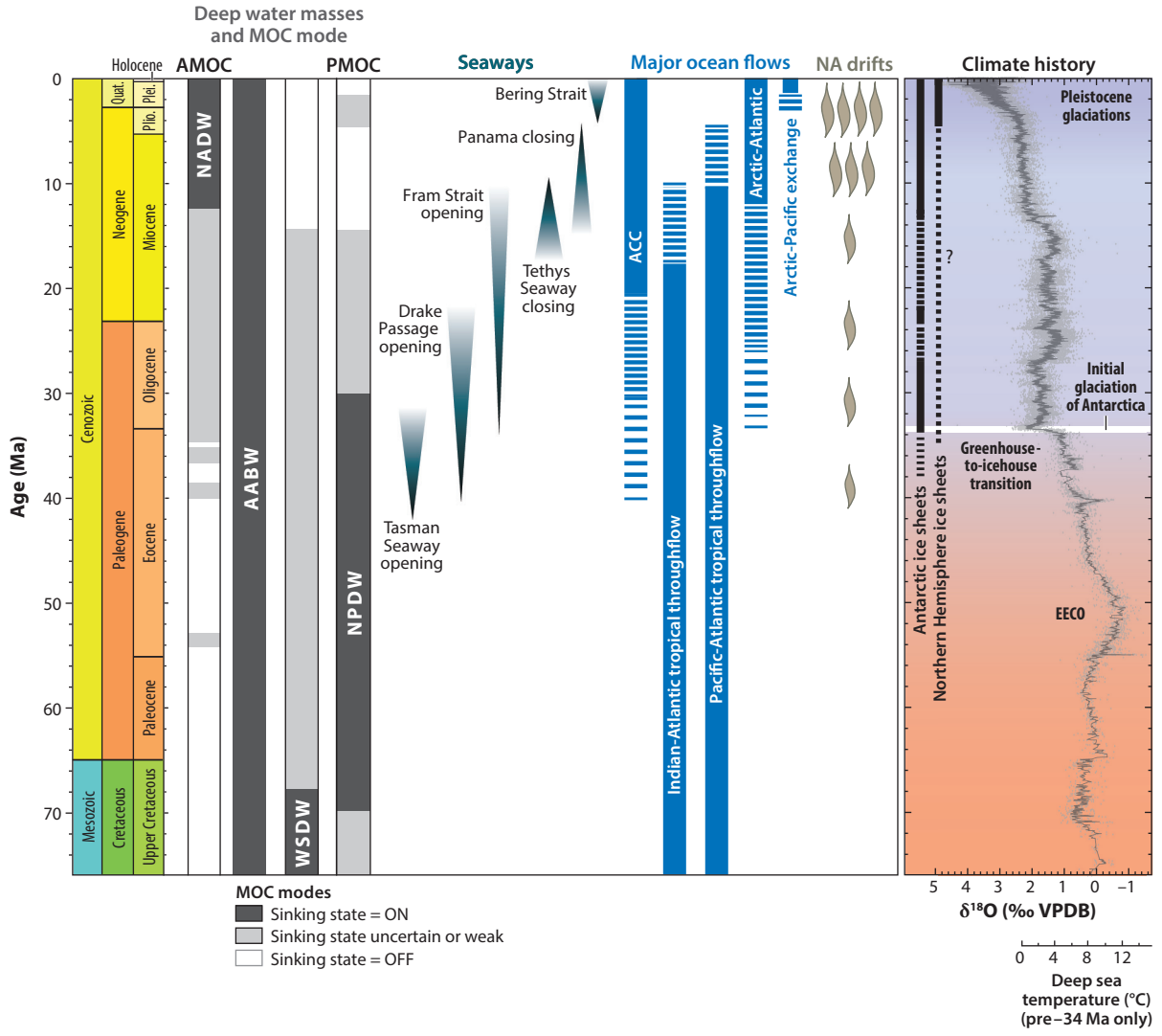

Figure 3

A history of global MOC since the Upper Cretaceous based on geological data and models. Water masses are named after their formation sites and eventual depth and not their water mass properties as is sometimes the convention. The elongated triangles represent the gradual nature of, and uncertainty in, the timing of tectonic gateway opening and closure. For the ocean flows, dashed segments signify phases when flows were weak or uncertain. "NA drifts" refers to deep-sea sedimentary drift deposits (i.e., sedimentary piles created by strong bottom-flowing currents) close to locations of NADW formation. The climate history (*right panel*), which emphasizes the transition from a greenhouse to an icehouse climate, is based on a compilation of deep-sea oxygen stable isotope ($\delta^{18}O$) records (Zachos et al. 2001, Cramer et al. 2009). The white line indicates glacial inception on Antarctica ~34 Ma. The $\delta^{18}O$ bottom water temperature scale was calculated for an ice-free ocean and, therefore, applies only to the time before Antarctic glaciation; thereafter, the $\delta^{18}O$ variability includes changes in global ice volume. Abbreviations: AABW, Antarctic Bottom Water; ACC, Antarctic Circumpolar Current; AMOC, Atlantic meridional overturning circulation; EECO, Early Eocene Climatic Optimum; MOC, meridional overturning circulation; NA, North Atlantic; NADW, North Atlantic Deep Water; NPDW, North Pacific Deep Water; Ma, million years ago; PMOC, Pacific meridional overturning circulation; VPDB, Vienna Pee Dee Belemnite; WSDW, Warm Saline Deep Water.

2.1. Distribution of Deep Water Formation Regions in the Geological Past

WSDW: Warm Saline Deep Water

NADW: North Atlantic Deep Water

A sensible place to start is the Upper Cretaceous [about 70 million years ago (Ma)] when an interhemispheric Atlantic Ocean was established (Thiede 1979, Murphy & Thomas 2013). At this time, the southern continents were attached to Antarctica, and a deep tropical oceanic corridor connected all the major basins. Upper Cretaceous data and models support deep water formation in numerous locations, including low-latitude regions [producing Warm Saline Deep Water (WSDW)], southern high-latitude regions, and the North Pacific (Brass et al. 1982, Cramer et al. 2009, Voigt et al. 2013, Thomas et al. 2014, Moiroud et al. 2016). This multilocation deep convection continued into much of the early Cenozoic (65–34 Ma). By 45 Ma, the Rocky Mountains had reached their modern elevation, helping to block some moisture transport from the Pacific to the Atlantic. However, there was still no sustained North Atlantic Deep Water (NADW) formation, although there may have been some intermittent pulses of NADW or North Atlantic Intermediate Water (Hohbein et al. 2012, Boyle et al. 2017).

The first evidence for some form of persistent AMOC appears around 34 Ma when Antarctica first developed a semipermanent ice cap and latitudinal thermal gradients increased sharply (Miller & Tucholke 1983, Wright & Miller 1993, Scher & Martin 2004, Via & Thomas 2006, Borrelli et al. 2014, Coxall et al. 2018). The onset of the AMOC has been separately explained by the critical widening of Drake Passage and the deepening of the Greenland-Scotland Ridge (Via & Thomas 2006, Borrelli et al. 2014, Abelson & Erez 2017). Both data and models support a scenario in which the North Atlantic was contributing deep water to some extent throughout the Oligocene and Miocene (thus from 34 Ma until 5 Ma) (Burton et al. 1997, Nisancioglu et al. 2003, Thomas & Via 2007, Herold et al. 2012). However, models tend to agree that a strong AMOC is unable to form in a warm climate and with tropical gateways open. Instead, the Southern Ocean and a possible PMOC dominate (Mikolajewicz et al. 1993, Herold et al. 2012, Yang et al. 2014).

The modern AMOC developed in two stages. The first stage was during the late Miocene (12–9 Ma) as tropical seaways were in the final stages of closure. Data and model support for a PMOC disappears at this time (Woodruff & Savin 1989, von der Heydt & Dijkstra 2006, Yang et al. 2014). A second stage of intensification of NADW has been postulated to coincide with the onset of full-scale glacial cycles in the late Pliocene–early Pleistocene (~4–3 Ma) (Wright & Miller 1993, Burton et al. 1997, Bell et al. 2015, Boyle et al. 2017). These late Cenozoic AMOC adjustments happened at the time of the eventual sealing of the Panama Strait and the opening of the Bering Sea Arctic-Pacific passages. Several studies suggest that this period of AMOC intensification coincided with stratification of the North Pacific (Studer et al. 2012) and the cessation of deep water formation there (Kwiek & Ravelo 1999, Burls et al. 2017). Importantly, the postulated strengthening of an AMOC together with the weakening of a PMOC occurred under basin configurations similar to those of today, and as a result of climate change rather than tectonic changes.

2.2. The Quaternary: Glacial-Interglacial Cycles

Since its establishment, the AMOC has been a persistent, if variable, feature of the Plio-Pleistocene ocean (Raymo et al. 2004). In contrast, there is little evidence for a deep PMOC during the Plio-Pleistocene (Keigwin 1987, Raymo et al. 1990, Lynch-Stieglitz & Fairbanks 1994). Instead, there is the suggestion of greater intermediate-depth (<2 km) ventilation in the North Pacific during the last ice age and particularly during deglacial millennial oscillations (Okazaki et al. 2010, Rae et al. 2014, Freeman et al. 2015). During interglacial intervals, the deep Atlantic basin has generally been filled to ~4 km water depth or more with nutrient-depleted waters of North Atlantic origin (Duplessy et al. 1988, Raymo et al. 1990, Curry & Oppo 2005). During glacial intervals, the deep

Atlantic appeared much more like the deep Pacific (Boyle & Keigwin 1985, Raymo et al. 1990), with similar waters, presumably of southern origin, filling the depths of both basins and AMOC shoaling to intermediate depths above ~2.5 km (Curry & Oppo 2005, Lynch-Stieglitz et al. 2007). Recent evidence also suggests the presence of a limited amount of glacial AMOC to truly abyssal depths (Keigwin & Swift 2017). There is extensive evidence for the shallower glacial AMOC from multiple indicators, including dynamical proxies that suggest a relatively vigorous overturning cell (McCave et al. 1995, Gherardi et al. 2009, Lippold et al. 2012). Late Pleistocene deglacial transitions were marked by dramatic, transient weakening of the AMOC, characterized by the reduction and additional shoaling of the northern overturning cell before its rejuvenation at the onset of the ensuing interglacial interval (Boyle & Keigwin 1987, McManus et al. 2004, Robinson et al. 2005). Based on evidence from the most recent glacial inception, transitions into glacial intervals may have been accompanied by a temporarily strengthened AMOC (McManus et al. 2002, Guihou et al. 2011). Millennial variability in the overturning rate and depth of the AMOC characterized the last ice age, with particularly dramatic reductions associated with catastrophic iceberg discharge events (Curry et al. 1999, Böhm et al. 2015, Burckel et al. 2015, Henry et al. 2016). Previous glacial intervals may have been marked by similar variability (McManus et al. 1999). While the interglacial AMOC appears to be more robust, perhaps due to reduced meltwater from circum-Atlantic ice (McManus et al. 1999), there is evidence of muted millennial variability in the Holocene (Oppo et al. 2003, Thornalley et al. 2013, Eldevik et al. 2014) and possibly greater variability within the preceding interglacial interval (Galaasen et al. 2014, Mokeddem et al. 2014).

3. ATMOSPHERIC INFLUENCES ON THE ATLANTIC-PACIFIC ASYMMETRY

3.1. Atmospheric Forcing of Ocean Salinity

The atmospheric controls on near-surface salinity can be divided into a direct forcing via freshwater fluxes and indirect influences (e.g., the wind-driven circulation and salinity advection). Differences in both factors may contribute to the Atlantic-Pacific salinity contrast (Warren 1983, Broecker et al. 1985, Zaucker et al. 1994, Emile-Geay et al. 2003, de Boer et al. 2008, Czaja 2009, Ferreira et al. 2010, Wills & Schneider 2015, Craig et al. 2017).

The steady-state balance for salinity S averaged over the upper ocean to depth H can be summarized symbolically as (e.g., Ponte & Vinogradova 2016, Busecke et al. 2017)

$$A + D + \frac{B}{H} = S\frac{\widetilde{P}}{H}, \qquad 1.$$

where A and D represent average advective and diffusive salinity fluxes into the ocean column, respectively, either horizontally through the sides or vertically through the bottom; B represents a salt flux associated with sea-ice formation/melting, which is important only in polar regions; and $\widetilde{P} = P - E + R = -\nabla \cdot M$ is the atmospheric freshwater forcing from $P - E$ and river runoff R, which are balanced by convergence of moisture fluxes M in the overlying atmospheric column and adjacent catchment areas (**Figure 4*a***).

The strength of atmospheric freshwater forcing $\widetilde{P}$ is negatively correlated with the upper-ocean salinity S across different ocean regions (**Figure 4*c***). In the zonal mean, the freshwater forcing is positive in the intertropical convergence zone, where precipitation exceeds evaporation; negative in the subtropics, where evaporation exceeds precipitation; and positive at high latitudes. Zonal anomalies such as the Asian monsoon outflow over the Pacific modulate the zonal-mean patterns regionally (**Figure 4*a***). The salinity distribution reflects these forcing contrasts (**Figures 2*a*** and

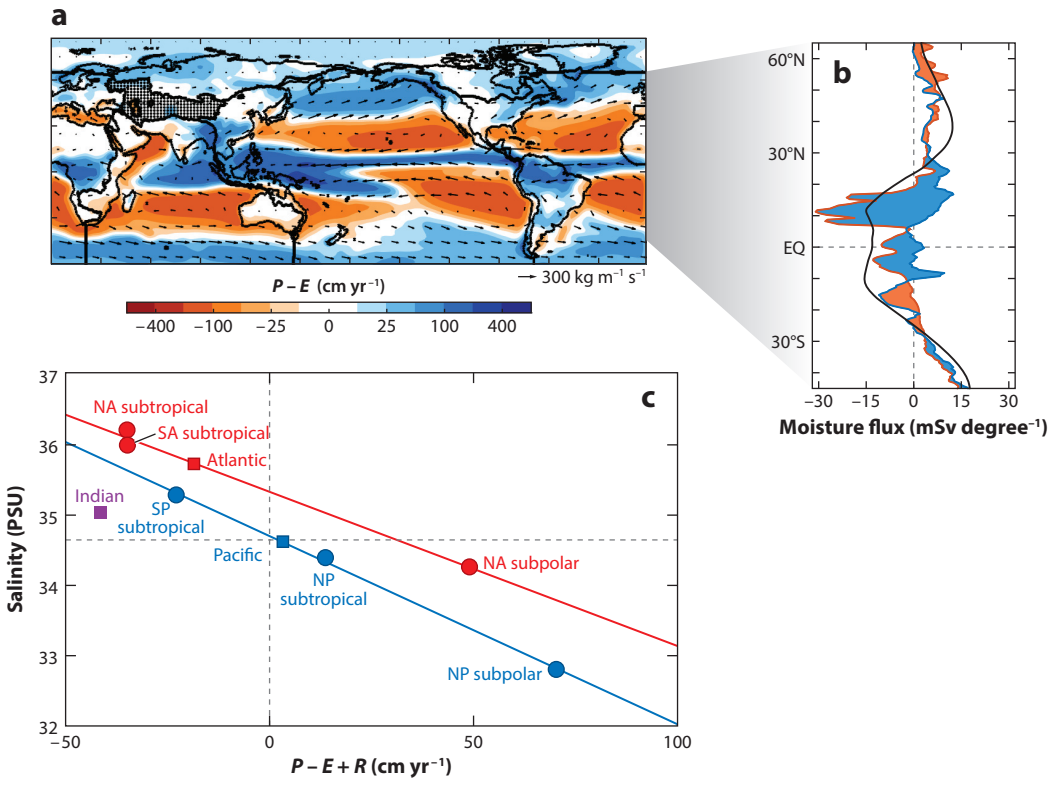

Figure 4

(*a*) Net precipitation $P - E$ (*shading*), vertically integrated moisture fluxes (*arrows*) from ERA-Interim reanalysis for 1979–2012 (Dee et al. 2011), and drainage boundaries (*thick solid lines*; Vörösmarty et al. 2000). The contours are such that each contour represents a factor-of-2 increase in $P - E$; values less than 12.5 cm yr^{-1} are in white. Stippling represents endorheic basins. (*b*) Moisture transport (smoothed with a 2° running average) into the Pacific basin across the western boundary from Asia and the Indian Ocean (*blue line*) and out of the Pacific basin across the eastern boundary into the Americas and the Atlantic (*orange line*). Net freshwater input to the Pacific is the difference between these lines; it is colored blue when positive and orange when negative. Both zonal and meridional moisture fluxes are included in the calculation. The continental divides are used as boundaries so that rivers that drain into the Pacific are included. A solid black line shows the zonal-mean zonal moisture transport (same at each ocean boundary). (*c*) Mean sea surface salinity from the *World Ocean Atlas 2013* (Zweng et al. 2013) versus freshwater forcing for the Atlantic (including the Mediterranean), Pacific, and Indian Oceans between 40°S and 65°N, as wholes (*squares*) and split up geographically into regions (*circles*): North Atlantic (NA) and North Pacific (NP) subpolar gyres (40°N–65°N) and subtropical gyres (0°–40°N) and South Atlantic (SA) and South Pacific (SP) subtropical gyres (0°–40°S). Least-squares lines are computed separately for the Pacific (*blue*) and Atlantic (*red*).

4*c*), for example, with higher salinity in subtropical than in subpolar ocean basins. Salinity decreases by about 1 PSU for every 40 cm yr^{-1} increase in $\widetilde{P}$. Interestingly, the individual gyres of the Atlantic and Pacific appear to fall onto separate lines on the S versus $\widetilde{P}$ plot (**Figure 4*c***). The lines are separated by about 0.6 PSU, reflecting differences in salt transport at the basin boundaries (i.e., the Southern and Arctic Oceans). The slope of the line is shallower in the Atlantic, indicating more efficient meridional salt transport and mixing in the Atlantic.

3.2. Asymmetry in Atmospheric Freshwater Forcing

Overall, differences in freshwater input account for about half of the average Atlantic-Pacific salinity contrast of 1.1 PSU (**Figure 4*c***), with an average of 22 cm yr^{-1} more freshwater input in

the Pacific than in the Atlantic (**Figure 4*b***), or a net difference in freshwater input of 0.4 Sverdrups (Sv) over 35°S–60°N (an estimate that is robust across data sets; see Craig et al. 2017). Moisture transports by atmospheric eddies and monsoonal circulations are primarily responsible for this freshwater forcing asymmetry.

Sverdrup (Sv): a unit of volume transport; 1 Sv = 10^6 m^3 s^{-1}

Moisture transport by atmospheric eddies. Atmospheric stationary eddies and zonally anomalous circulations are the main drivers of $P - E$ contrasts between ocean basins (Wills & Schneider 2015). Stationary eddies are driven by orography and zonal variations in atmospheric heating, leading to net precipitation anomalies where there is low-level convergence of air masses. For example, Asian orography and the atmospheric heating over the warm pool drive stationary Rossby waves, which generate the Aleutian Low over the North Pacific (Sardeshmukh & Hoskins 1988). This contributes to zonally anomalous net precipitation over the North Pacific that is 21 cm yr^{-1} higher than in the North Atlantic (**Figure 4*c***). As another example, stationary eddies are responsible for the zonally anomalous moisture convergence downstream of Tibet (Molnar et al. 2010), which leads to a net precipitation anomaly over East Asia and the South China Sea, contributing to the net moisture transport into the Pacific basin (**Figure 4*b***). Consistent with the importance of stationary eddies for $P - E$ contrasts, some climate models show a decrease in AMOC and an increase in PMOC when mountain ranges are removed (Schmittner et al. 2012, Sinha et al. 2012).

Atmospheric transient eddies (synoptic weather systems) also contribute to the Atlantic-Pacific contrast in freshwater forcing. While their contribution to the overall basin-mean contrast is small, the transient-eddy moisture flux convergence is locally 14 cm yr^{-1} higher in the North Pacific subpolar gyre than in the North Atlantic subpolar gyre (Wills & Schneider 2015). Thus, transient eddies contribute to the salinity asymmetry at high latitudes. Zonal contrasts in transient-eddy moisture flux convergence arise in several ways. For example, there is intense evaporation close to the coast in winter, where cold continental air is advected over warm but narrow western boundary currents (Frankignoul 1985). This leads to a larger average evaporation rate per unit area in a narrower ocean basin, such as the Atlantic, than over a wider basin, such as the Pacific (Schmitt et al. 1989). Additionally, there is a fetch on the order of the decorrelation length of transient eddies (~3,000 km) before moisture evaporated close to the coast is returned to the surface as precipitation, promoting enhanced eastward atmospheric moisture export from a narrower basin (Ferreira et al. 2010). These and other effects may set the zonal contrasts in the transient-eddy moisture flux convergence between the Atlantic and Pacific.

Zonal moisture transport by monsoonal circulations and across Panama. It has been proposed that zonal moisture transport across the Isthmus of Panama is a primary mechanism for freshening the Pacific (Zaucker et al. 1994, Emile-Geay et al. 2003, Leduc et al. 2007). Indeed, between around 15°S and 20°N (including the latitude of Panama), the atmosphere transports moisture into the Pacific basin across the eastern boundary (**Figure 4*b***). However, this moisture transport is close to that which would be accomplished by the zonal-mean easterly winds alone (**Figure 4*b***). What matters for salinity contrasts is differential zonal moisture transport across the eastern and western boundaries of basins. The atmosphere between 5°N and 25°N also transports moisture into the Pacific across the western boundary. Here, the zonal-mean easterlies alone would lead to moisture export. The anomalous moisture import across the western boundary is a result of the Asian monsoon outflow (**Figure 4**), which transports moisture into the tropical and subtropical Pacific (Emile-Geay et al. 2003). So while moisture transport across Panama does freshen the Pacific, the net freshening arises because zonally anomalous monsoonal circulations prevent the moisture from leaving the Pacific basin across its western boundary. One result of

this Atlantic-Pacific asymmetry is that the subtropical North Pacific (0°–40°N) experiences positive freshwater forcing ($\widetilde{P} > 0$), whereas the subtropical North Atlantic experiences negative freshwater forcing ($\widetilde{P} < 0$) (**Figure 4*c***) (see also Czaja 2009).

3.3. Asymmetries in Wind-Driven Ocean Circulations

The freshwater forcing contrasts between ocean regions force salinity contrasts, which the advective and diffusive ocean fluxes A and D balance and moderate (Ponte & Vinogradova 2016). If the net effect of A and D on large scales is to relax salinity contrasts ΔS on a mixing timescale T such that $A + D \sim \Delta S/T$, then the salinity balance (Equation 1), neglecting sea-ice fluxes B, implies that a fractional salinity contrast $\Delta S/S$ resulting from the freshwater forcing contrast needs to be balanced by salinity mixing on a timescale

$$T \sim \frac{\Delta S}{S}\frac{H}{\Delta \widetilde{P}}, \qquad 2.$$

where H is the depth of the relevant water column. For the north-south freshwater forcing contrast of $\Delta \widetilde{P} \sim 0.5$ m yr^{-1} between the subtropics and high latitudes (**Figure 4*c***) and the corresponding fractional salinity contrast $\Delta S/S \sim 5\%$ (**Figures 2** and **4*c***), assumed to extend over a depth $H \sim 500$ m, the salinity mixing timescale is $T \sim 50$ yr, consistent with inferences from data and models (Zika et al. 2015). Lateral eddy mixing is too weak to supply the required salinity mixing (Busecke et al. 2017). However, wind-driven ocean circulations such as gyres and their seasonal and interannual variations and/or shallow overturning circulations can plausibly transport and mix salinity on decadal timescales, as they do with heat (Talley 2003, Boccaletti et al. 2005).

Differences in transport and mixing between the Atlantic and Pacific may amplify or dampen the salinity contrasts between the two basins induced by freshwater forcing. The relation (Equation 1) for the salinity mixing timescale implies $\Delta S/S \sim \Delta \widetilde{P} T/H$; that is, for fixed H, the timescale T is proportional to the slope of the lines in **Figure 4*c***. Hence, the shallower slope of the $S - \widetilde{P}$ line for the Atlantic than for the Pacific indicates that the Atlantic has a somewhat (∼20%) shorter mixing timescale than the Pacific. This may arise, for example, because of the existence of the AMOC (e.g., Stommel 1961), or because the surface westerlies are more variable over the Atlantic, driving greater variability of ocean gyres (Eichelberger & Hartmann 2007, Czaja 2009). One effect of the more efficient mixing in the North Atlantic is that subpolar salinities are further enhanced over those in the North Pacific because saline subtropical waters are more effectively mixed poleward, fostering deep convection in the subpolar North Atlantic.

3.4. Discussion and Implications

Contrasts in atmospheric moisture flux convergence, and hence in freshwater forcing, between the Atlantic and Pacific primarily arise because of atmospheric stationary eddies and monsoonal circulations. It has been suggested that ocean dynamics such as the AMOC also modulate evaporation, e.g., through the advection of warm waters that enhance evaporation (Warren 1983, Broecker et al. 1985, Czaja 2009). However, such evaporation modulations would have to affect atmospheric moisture transport (e.g., by driving stationary waves) to lead to changes in net precipitation $P - E$. Otherwise they would merely lead to compensating local precipitation modulations, without an effect on freshwater forcing. For example, while global temperature increases do enhance evaporation, they generally also lead to enhanced net precipitation $P - E$ over ocean regions where $P - E > 0$, such as the subpolar gyres. That is, the evaporation increase is regionally overcompensated by a precipitation increase (e.g., Held & Soden 2006, Durack et al. 2012). Thus,

it is not clear whether AMOC-induced warming that is confined to latitudes poleward of 20°N (**Figure 2*b***) necessarily leads to reduced $P - E$ over the Atlantic, or how large that effect may be.

4. LOCAL OCEANIC DETERMINANTS

To further understand the Atlantic-Pacific asymmetry, it is useful to study controls on the occurrence (or absence) of deep convection at the local scale of the Atlantic or Pacific basin.

4.1. Convection and the Role of Salinity

Deep convection happens when the surface becomes denser than the underlying deep water, producing static instability. This occurs only in regions already weakly stratified, i.e., the Southern Ocean, North Atlantic, and North Pacific (**Figure 5*a***). One might therefore expect that deep convection could happen in both northern basins.

However, the nonlinearity of the seawater equation of state provides a fundamental constraint. To a good approximation, seawater density varies linearly with salinity but quadratically with temperature (e.g., Roquet et al. 2015). The thermal expansion coefficient varies by one order of magnitude between the tropics and the poles, such that density variations in near-freezing waters are insensitive to temperature and are dominated by salinity variations. This nonlinearity dramatically amplifies the impact of the salt contrast between the Atlantic and Pacific basins (**Figure 5**). The temperature effect on stratification is comparable between the two basins, weakening northward (**Figure 5*b***). But the salinity effect exhibits a large asymmetry (**Figure 5*c***): It significantly stabilizes the upper ocean in the Pacific but only weakly stabilizes the Labrador Sea; it destabilizes the Nordic and Irminger Seas.

In warmer climates with higher polar ocean temperatures, the effect of the thermal gradients on density is higher. As a result, the haline-driven stabilizing density gradients in the fresh polar regions become less important and the preference of sinking in the Atlantic less pronounced (de Boer et al. 2007, 2008; Sigman et al. 2004). Indeed, a number of paleoproxies suggest enhanced ventilation in the Pacific and Southern Oceans (which currently have the strongest polar haloclines) in warmer climates when the continental configuration was similar to today's (e.g., ∼3 Ma; see Section 2).

4.2. The Role of Ocean Basin Geometry

Asymmetries in basin geometry may cause oceanic patterns of salinity and temperature advection that favor sinking in the Atlantic.

The narrower width of the Atlantic relative to the Pacific can create a preference for Atlantic sinking through interactions between the wind-driven gyre circulation and the MOC in the subpolar oceans (de Boer et al. 2008, Jones & Cessi 2016). An important effect is the different dependencies on basin width of the meridional western boundary volume transports associated with the MOC and the wind-driven gyre (Jones & Cessi 2016). The wind-driven meridional gyre velocities are in Sverdrup balance in the interior basin and are set by the local wind stress curl (Sverdrup 1947), whereas the speed of swift western boundary currents increases linearly with basin width for a given wind stress (Stommel 1948). In contrast, the western boundary velocity associated with the MOC is, to first order, independent of the basin width, because the global MOC volume transport is controlled by Southern Ocean wind stress and global diapycnal upwelling (Gnanadesikan 1999, Jones & Cessi 2016) and is insensitive to the location of the geographically confined northern high-latitude sinking.

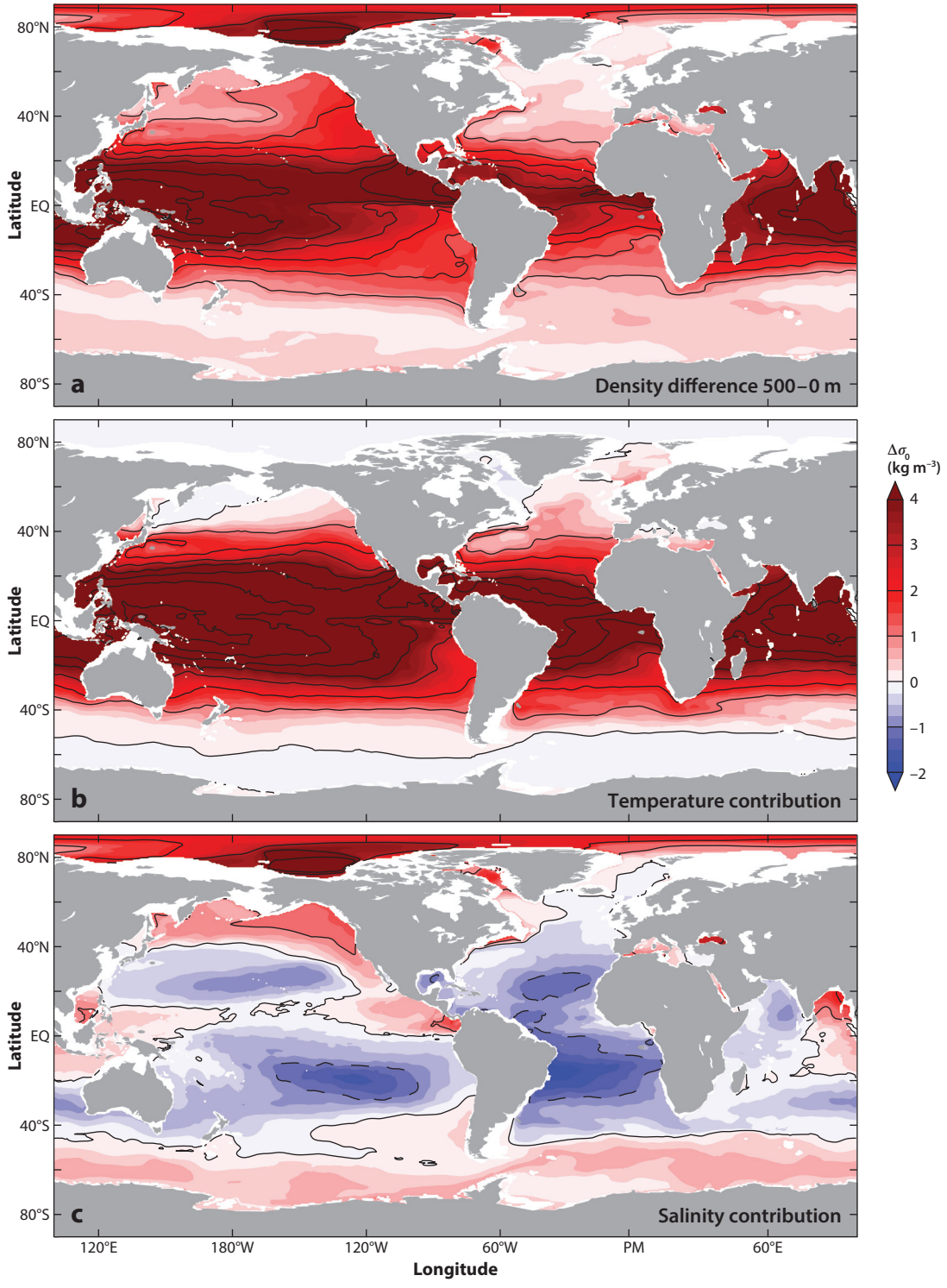

(*Caption appears on following page*)

Figure 5 (*Figure appears on preceding page*)

Upper stratification in the present-day World Ocean. (*a*) Potential density difference $\Delta\sigma_0$ between 500 m and the surface at the time of year when it is the smallest. The density difference can be decomposed linearly into (*b*) a temperature contribution $-\rho_0\alpha\Delta\theta$ and (*c*) a salinity contribution $\rho_0\beta\Delta S$, where α is the thermal expansion coefficient and β is the haline contraction coefficient.

The flow field in the upper ocean is essentially the sum of the wind-driven gyre circulation and the western boundary layer flow of the MOC. In the Northern Hemisphere subtropical (subpolar) gyre, the western boundary layer velocities of the wind-driven circulation and of the MOC reinforce (counteract) each other. In the subpolar gyre, this interaction gives a smaller northward transport in the western boundary layer from the subtropical to the subpolar region in a wide basin relative to a narrow basin. This difference implies that, near the high-latitude sinking, freshwater from the north is more efficiently transported southward and into the central basin in the North Pacific relative to the North Atlantic, contributing to the formation of a strong halocline in the subpolar North Pacific that is absent in the North Atlantic (Jones & Cessi 2016).

The more northerly extension of the Atlantic has also been invoked as a potential contributor to the North Atlantic sinking. This effect was observed in modeling studies (de Boer et al. 2008, Huisman et al. 2012), although the exact mechanism at play remains to be clarified.

Exchanges through seaways and straits may also influence deep water formation by controlling the supply of freshwater to the convective zones. On the paleoclimate scale, opening and closing of passages may have altered the preference for AMOC and PMOC states. The Bering Strait, for example, makes the AMOC weaker than it would be with a closed Bering Strait (e.g., Hu et al. 2012). A weaker AMOC leads to a reduction or reversal of freshwater input from the Pacific to the Atlantic through the Bering Strait and thereby provides a negative feedback that stabilizes the AMOC (de Boer & Nof 2004, Okumura et al. 2009). Proxy evidence suggests that the North Pacific Intermediate Water formation was stronger during strong glacials, and this was attributed to the closing of the Bering Strait during strong glacials because of sea-level drop (Knudson & Ravelo 2015).

Finally, the effect of the highly evaporative Mediterranean Sea was one of the earliest explanations for the presence of an AMOC. Reid (1979) argued that the Mediterranean outflow feeds into the Nordic Seas, helping to maintain high salinities in convective sites. However, recent studies arrive at inconsistent conclusions on whether the Mediterranean outflow contributes, by mixing, to the salinification of the upper limb (Blanke et al. 2006) or of the lower limb (Jia et al. 2007) of the AMOC. More critically, the net $P - E$ over the Mediterranean Sea explains only a small contribution of the Atlantic $P - E$ (about -0.05 Sv out of -0.4 Sv over the Atlantic). It is not clear whether the enclosed sea adds anything more than the net $P - E$ it receives.

4.3. Local Feedbacks

Once the MOC is in place, local feedbacks may help maintain its location. As illustrated by the Atlantic (**Figure 2*b***), the convective basin tends to be relatively warmer as the MOC converges heat toward the convection zone. Higher temperatures decrease the surface density (negative feedback). It has been suggested that they favor higher evaporation rates (Warren 1983), which increase the salinity and hence the density (positive feedback), but that presupposes that higher evaporation rates are not locally compensated by enhanced precipitation, as they may be (Section 3). The net result of these effects is unclear. It is possible that the salinity effect dominates through the nonlinearity of the equation of state and that the net heat-advection feedback is positive. This may, however, change in a warmer climate.

A second local positive feedback is the convective salt feedback discussed in Welander's model of convective mixing (Welander 1986). Once convection stops, freshwater accumulates near the surface in regions of net freshwater input, which inhibits further convection. A second element of this feedback is that because of net freshwater input at the surface, convective mixing is associated with upward mixing of salt, leading to further freshening when convective mixing decreases. This feedback may be most effective in the Labrador Sea, where the density stratification is weak, and may explain abrupt transitions in Labrador Sea convection in climate models forced with anthropogenic change scenarios (Sgubin et al. 2017).

5. NONLOCAL OCEANIC DETERMINANTS

A self-sustaining mechanism in which the MOC localizes deep convection in the basin it occupies may contribute to the Atlantic's salinity and permit multiple equilibria of the AMOC. This behavior, which can be formalized using Stommel's (1961) ideas, requires a global perspective, notably because of the central role of freshwater exchanges between the Atlantic and the rest of the ocean.

5.1. Active Ocean: The Salt-Advection Feedback

Stommel's (1961) two-box model accounts for the competition between thermal and haline contributions to the density of water. Although not originally designed with the large-scale circulation in mind, the two boxes are often interpreted as the low-latitude and high-latitude oceans (Rooth 1982, Rahmstorf 1996). In the model's simplest form, temperatures are prescribed and salinity is forced by a virtual surface salt flux. While the flux acts to enhance the salinity contrast between the boxes, advection (AMOC) decreases it. The circulation between the boxes is a function of their density difference [a simple parameterization that finds support in some ocean general circulation models (e.g., Thorpe et al. 2001) but not in others (e.g., de Boer et al. 2010, Wolfe & Cessi 2010)]. For moderate freshwater forcing, there are two stable equilibria. The first stable equilibrium (the ON state) corresponds to a fast circulation (small mixing time T in Equation 2) with high-latitude sinking and with the density gradient dominated by the temperature gradient between the boxes, set by the atmospheric forcing. In contrast, the second stable equilibrium (the OFF state) corresponds to a slow circulation (large mixing time T) with a salt gradient that overcomes the temperature gradient in its effect on density, and sinking occurs in the equatorial box. The mechanism by which the flow makes transitions from one equilibrium to another is the salt-advection feedback. A freshwater anomaly in the high-latitude box leads to decreased flow through a reduction in the density difference between the two boxes, and hence to reduced salt advection from the low-latitude box that amplifies the initial anomaly.

Importantly, in more complex geometries, Stommel's mechanism can sometimes result in a PMOC solution, in isolation or with other cells. Marotzke & Willebrand (1991) (see also Bryan 1986) found four equilibria in a low-resolution ocean model under an equatorially symmetric heat and freshwater forcing: a northern sinking state, a southern sinking state, a conveyor state, and an inverse-conveyor state. In some models with realistic configurations, a PMOC may arise in response to freshwater hosing in the Atlantic, although this is sensitive to how the North Atlantic freshwater hosing is compensated elsewhere in the global ocean (Jackson et al. 2017). This leads to a natural follow-up question: Does the real climate system possess multiple MOC equilibria?

Observations provide few clues to address this question. Despite being frequently invoked in the context of past abrupt climate changes, an AMOC OFF state is not supported by paleoproxies, which rather point toward a weakened AMOC state and only sporadic/weak ventilation in the North Pacific (Section 2). Evidence for multiple states in the present climate is also unclear.

Simple models suggest that multiple equilibria can exist only when the overturning circulation exports freshwater from the Atlantic (Rahmstorf 1996, de Vries & Weber 2005, Dijkstra 2007). In this case the salt-advection feedback is destabilizing: A weakening of the MOC leads to a freshening of the basin and further weakening of the MOC. In practice, the freshwater transport by the AMOC in the Atlantic, often denoted F_{ov}, is difficult to estimate and is usually approximated by the freshwater transport by the zonally averaged circulation, which includes components of the ocean circulation other than the MOC (e.g., Ekman currents). Nonetheless, estimates based on observations point to a negative F_{ov} (Garzoli et al. 2013); i.e., the MOC exports freshwater, suggesting a possibly bistable regime.

Evidence from models is also inconclusive. While hysteresis of the MOC is commonly found in freshwater hosing experiments in coarse ocean-only and intermediate-complexity coupled models (e.g., Rahmstorf et al. 2005), it seems to disappear in more complex climate models (e.g., Stouffer et al. 2006). However, MOC hysteresis has reappeared in the latest models with eddy-permitting ocean components (although the OFF state resembles the weak and shallow mode prevailing during glacial maxima; Mecking et al. 2016). The stability of the AMOC in the coupled system remains an open question, but the succession of model generations has revealed potential feedbacks in the atmosphere (e.g., Yin & Stouffer 2007) and the ocean (Mecking et al. 2016), challenging the central role of F_{ov} in determining this stability.

Assuming multiple equilibria exist, is the present state one of a few equally possible states, or is it favored by the present-day forcing and geometry? As highlighted in this review, there are many asymmetries between the Atlantic and Indo-Pacific basins. Once symmetry is broken, a single cell appears to be the preferred mode of overturning. The circulation in this single cell is global: Sinking occurs in the high latitudes of the Northern Hemisphere in one basin, and upwelling occurs in all sectors along the circumpolar region and globally (through diapycnal mixing at the interface between the deep and abyssal cells around 2,000 m depth; see Talley 2013). Huisman et al. (2012) determined the solution structure in a global ocean model and suggested that continental geometry is a very efficient selection mechanism, such that even when the Atlantic is forced by net precipitation, an AMOC with an Atlantic sea surface salinity that resembles the present-day salinity field can still exist.

5.2. Salt Exchanges with the Southern Ocean and Pathways Within the Atlantic

A salient feature of the present-day ocean basin geometry is the Southern Hemisphere latitude band where the South American continent provides the western as well as the eastern boundary for a common sector shared by the Atlantic and Indo-Pacific Oceans, which is terminated northward by the southern tip of Africa. This general geometric feature with a circumpolar Southern Ocean intercepted northward by one long (America) and one short (Africa) continent yields an interplay between the wind-driven gyre circulation and the MOC that creates asymmetries in the characteristics of the water masses feeding the upper limb of the AMOC. Water masses entering the Atlantic from the east, around the short continent via the Agulhas leakage, are warm/salty Indian Ocean thermocline waters (the Warm Route; Reid 1961, Gordon 1986). Water masses entering the Atlantic from the west, with the Antarctic Circumpolar Current (long continent), are of subpolar origin (sub-Antarctic and intermediate waters) and tend to be fresh and cold (the Cold Route; Rintoul 1991).

The relative contributions of these two routes remain debated (Speich et al. 2001, Donners & Drijfhout 2004, Beal et al. 2011). From the freshwater budget and stability points of view, however, the important characteristic is the salinity of the water masses that feed the upper limb, rather than the geographical pathways that brought them there (Lohmann 2003).

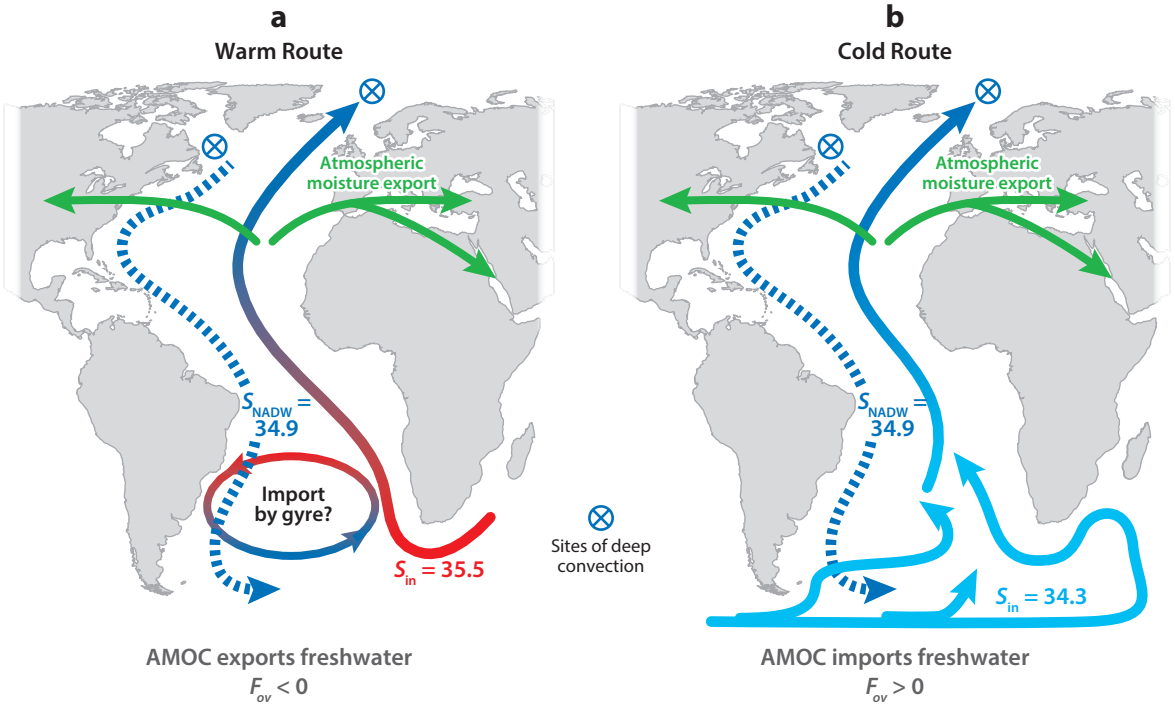

Figure 6

Schematic of the Warm and Cold Routes and their implication for the basin-wide freshwater budget and stability of the AMOC. (*a*) In the Warm Route case, waters (*red–blue arrow*) get fresher as they are transported northward, so the deep return flow (*dashed blue arrow*) is fresher than the upper branch; the AMOC exports freshwater in the basin. (*b*) In the Cold Route case, the AMOC is fed by the cold (fresh) waters that get saltier as they are transported northward, consistent with a net evaporation over the Atlantic basin; the AMOC imports freshwater. The blue crossed circles indicate sites of deep convection. Abbreviations: AMOC, Atlantic meridional overturning circulation; F_{ov}, freshwater transport by the Atlantic meridional overturning circulation; NADW, North Atlantic Deep Water; S_{in}, salinity of the water masses entering the Atlantic basin; S_{NADW}, salinity of the North Atlantic Deep Water.

In the Warm Route scenario, the export of NADW out of the Atlantic is balanced by input of water masses saltier than the NADW (**Figure 6*a***). The AMOC therefore exports freshwater out of the Atlantic basin, which corresponds to a negative F_{ov} and potential bistability of the AMOC. As the Atlantic basin is also a net evaporative basin (Section 3), closure of the freshwater budget requires a large freshwater input into the basin by a process other than the AMOC. The wind-driven South Atlantic subtropical gyre and eddy mixing are potential candidates (Rahmstorf 1996, de Vries & Weber 2005). In the Cold Route scenario (Broecker 1991), the NADW export is compensated by low-salinity water (**Figure 6*b***). The AMOC therefore imports freshwater into the Atlantic basin (a positive F_{ov}, indicating a stable regime). In this case, the Atlantic freshwater budget is readily balanced by the net evaporation and atmospheric export to the Indian and Pacific Oceans.

A fundamental question is how the Agulhas salt transport into the South Atlantic depends on the continental configuration and the wind field. Numerical experiments combined with insights from classical theory of wind-driven gyre circulation (Sverdrup 1947, Stommel 1948) show that this issue depends critically on the southward extents of the African and American continents relative to the surface wind stress field. Reid (1961) was one of the first to make the connection

between the long/short continent asymmetry and the elevated salinity of the Atlantic Ocean. He argued that the current distribution of winds and zonal continental boundaries favors the Warm Route over the Cold Route.

Using a global ocean-circulation model, Sijp & England (2009) showed that the AMOC intensifies when the Southern Hemisphere wind field is shifted southward, which enhances the Agulhas leakage and the warm water path contribution to the AMOC. Conversely, when the wind field is shifted northward, the Agulhas leakage and the AMOC decrease, whereas in the Pacific the salinity and the northern intermediate-depth overturning cell increase.

Numerical experiments in which the southward extents of the two continents, rather than the wind field, are shifted latitudinally have provided additional insights into how winds and geometry influence the location of deep sinking (Nilsson et al. 2013, Cessi & Jones 2017). Using an idealized Atlantic-Pacific configuration, Cessi & Jones (2017) showed that when the short "African" continent is northward (southward) of the zero wind stress curl line (near 45°S), the flow in the upper branch of the MOC from the Indo-Pacific to the Atlantic occurs preferentially through the Warm (Cold) Route. In these simulations, the Atlantic basin becomes significantly more saline (by 2 PSU at the surface) than the Indo-Pacific one, despite identical net surface freshwater flux in the two basins. The current configuration, with a short (long) continent on the eastern (western) boundary of the Atlantic, creates a southern subtropical supergyre that transfers salt from the Indo-Pacific to the Atlantic via the Warm Route (Gordon 1986).

Another fundamental question is how the Agulhas leakage and its impact on the Atlantic freshwater budget will change if the Northern Hemisphere deep water formation shifts to the Pacific Ocean. **Figure 7** illustrates such a scenario, which is based on coupled atmosphere-ocean model simulations in an idealized configuration with two equally wide basins and where the "African" and "American" continents terminate at 25°S and 50°S, respectively (Nilsson et al. 2013). This model allows for multiple equilibrium states: The Northern Hemisphere deep water

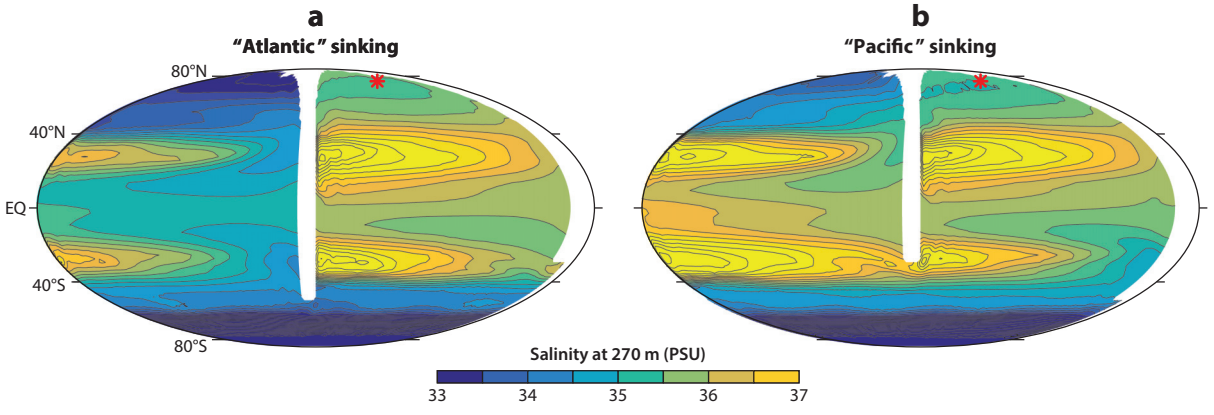

Figure 7

The thermocline salinity field (at 270 m) from a coupled ocean-atmosphere model configured on an ocean-covered Earth with two equally wide basins separated by two narrow continents terminating at 50°S and 25°S. A Mollweide projection, showing the full sphere, is used, and the second continent can be seen to the extreme right. In both cases, the sinking basin is depicted on the right (highlighted by a *red star*): (*a*) an equilibrium solution with sinking in the "Atlantic" basin with the long western boundary and (*b*) another equilibrium solution with sinking in the "Pacific" basin with the short western boundary. The salinity differences between the two states are mainly due to oceanic processes, as the basin $P - E$ differences are small. The figure also illustrates how the salinity field of the sinking basin is altered if the southward extents of "Africa" and "America" are interchanged; note that the ensuing salinity changes are most pronounced in the basin that does not form deep water. Model outputs from Nilsson et al. (2013).

formation can be located either in the basin with the long western boundary (AMOC) or in the basin with the short western boundary (PMOC). **Figure 7*b*** shows that the "Agulhas leakage" acts to make the Atlantic saline even in the presence of a PMOC. Thus, the "Agulhas leakage" salt transport operates partly independently of the AMOC and sets a preference for sinking in the "Atlantic" basin with the short eastern boundary.

6. MOVING FORWARD

Despite a series of recent theoretical and observational efforts to address the localization of deep water formation in the Atlantic, no clear answer has emerged. It is puzzling that such a fundamental aspect of Earth's climate remains so poorly understood.

As reviewed here, multiple factors appear to conspire in favor of Atlantic sinking, rather than Pacific sinking, in the present climate. These factors include the $P - E$ asymmetry, the different widths of the basins, and the meridional extent of the African and American continents. The $P - E$ asymmetry accounts for about half of the salinity contrast between the Atlantic and Pacific basins overall. Differences in salt transport across the basin boundaries, e.g., by the Agulhas leakage, may account for up to 30% of the salinity differences in subpolar regions (from the mean offset between the lines in **Figure 4*c***). The ∼20% shorter salinity mixing timescale in the Atlantic than in the Pacific accounts for an additional 20% of the salinity differences in subpolar regions (see **Figure 4*c***). Consistently, decreasing the $P - E$ asymmetry weakens the AMOC (e.g., Mecking et al. 2016), and increasing Agulhas leakage strengthens it (Beal et al. 2011). Yet, when the AMOC collapses, Agulhas leakage into the Atlantic still operates, although it is somewhat weaker (Laurian & Drijfhout 2011).

In numerical simulations, asymmetric sinking in the Atlantic can be achieved through ocean-only dynamics (e.g., with symmetric $P - E$ or even reversed $P - E$; see Huisman et al. 2012, Jones & Cessi 2016) as well as through atmosphere-only processes (e.g., through precipitation asymmetries; see Ferreira et al. 2010). The multiplicity of factors favoring sinking in the Atlantic over the Pacific would suggest that the present configuration of the global AMOC is a very stable situation. Yet paleoclimate proxies point to episodes of Pacific ventilation with a continental configuration similar to that of today. Critically, what drives the Atlantic-Pacific asymmetry now is not necessarily the same as what drove it in the past and what will drive it in the future. Changes in geography (through sea-level changes and continental drift) and the nonlinearity of the equation of state in warmer climates may dramatically alter the balance of drivers, resulting in fundamentally different regimes than today's. It is therefore unclear how inferences from past climates inform us about future climates.

Numerous studies provide very useful insights into the dynamical processes of the Atlantic-Pacific asymmetry, but they are difficult to reconcile. Part of the difficulty arises from the plethora of experimental setups used in previous studies, which has prevented meaningful comparisons of the relative importance of drivers. It is likely that multiple drivers are active simultaneously in the real world. But can we quantify their relative importance? Which ones are negligible and merely emerge in specific experimental setups?

To make further progress, we need to adopt a more quantitative approach. To this end, several strategies can be pursued simultaneously:

- Sensitivity tests with coupled ocean-atmosphere models represent our best chance to identify dominant drivers. Hypotheses need to be tested more systematically with general circulation models. Numerical experiments should be carried out using a coordinated modeling strategy. Sensitivity tests would include modifications of land topography, shape of ocean basins,

and air-sea feedbacks. Better quantifications of the driving processes of the Atlantic-Pacific asymmetry could provide a very useful framework to evaluate climate models.

- More detailed observations of the Atlantic freshwater budget are needed. Although observations permit closing of the basin-scale budget, sampling remains too sparse to allow a separation between processes (AMOC, eddies, gyres, etc.) and between pathways of the relevant water masses. Dynamically consistent, observationally constrained ocean state estimates are promising tools to better quantify the freshwater budget. In ocean models, the balance of the salt and freshwater budgets appears resolution dependent. Having a more robust quantification of the freshwater budget and salt pathways in the Atlantic would also serve as a useful reference to evaluate climate models.
- A possible fruitful avenue is an extensive feedback analysis of the AMOC or Atlantic freshwater budget. In modern coupled climate models, the basin-averaged Stommel feedback (characterized by F_{ov}) is not the only relevant feedback. An extended stability analysis (including atmospheric feedbacks, gyres, eddies, heat-advection feedback, etc.), as has been done in other contexts (see, e.g., Pithan & Mauritsen 2014 for Arctic climate feedbacks), would allow direct quantitative comparison of the various processes. A first attempt was made by den Toom et al. (2012) to include multiple feedbacks in a stability analysis.
- Quantification needs to be supported by theoretical models that represent crucial processes other than the MOC (e.g., eddy transport and gyres). This implies moving away from the conveyor belt/Stommel box model framework to adopt a more multifaceted and global view of the MOC (Talley 2013), including the role of the Southern Ocean and its eddy field (Marshall & Speer 2012). A first step in this direction has been provided by Johnson et al. (2007) by incorporating the salt-advection feedbacks of Stommel (1961) into the model of Gnanadesikan (1999).

In the future, net precipitation contrasts over oceans are expected to be enhanced under global warming (Held & Soden 2006). This in itself is expected to enhance the salinity contrast between the Atlantic and Pacific basins, as has been observed in the past decades (Durack et al. 2012) and as is simulated in climate change experiments (Levang & Schmitt 2015). However, enhanced net precipitation contrasts are accompanied by increased runoff from melting land ice, especially in the North Atlantic (Chen et al. 2006). Moreover, salinity differences between the two basins will likely have less impact on northern sinking as the climate warms, as seen in past climates. This is further complicated by the fact that these competing effects are acting on different timescales. Studies of future climate change scenarios have focused on the weakening of the AMOC, which seems dominated by surface heat flux changes (e.g., Gregory et al. 2005). They have not reported on the response of the North Pacific or the change in the Atlantic-Pacific asymmetry. How the Atlantic-Pacific asymmetry will evolve under global warming remains to be determined. The ongoing change may provide a crucial testing ground for our understanding of this important asymmetry in Earth's climate.

DISCLOSURE STATEMENT

The authors are not aware of any affiliations, memberships, funding, or financial holdings that might be perceived as affecting the objectivity of this review.

ACKNOWLEDGMENTS

We acknowledge funding from the International Meteorological Institute and the Bolin Centre for Climate Research for the workshop on "The Atlantic Meridional Overturning Circulation in

a Global Perspective" held at Stockholm University in September 2015. P.C., J.F.M., and T.S. acknowledge support from the US National Science Foundation (grant OCE-1634128 to P.C., grant AGS-1635019 to J.F.M., and grant AGS-1019211 to T.S.). T.E. acknowledges support from the Research Council of Norway (project NORTH). T.S. thanks Ryan Abernathey and Laure Zanna for helpful discussions.

LITERATURE CITED

Abelson M, Erez J. 2017. The onset of modern-like Atlantic meridional overturning circulation at the Eocene-Oligocene transition: evidence, causes, and possible implications for global cooling. *Geochem. Geophys. Geosyst.* 18:2177–99

Beal LM, de Ruijter PM, Biastoch A, Zahn R, SCOR/WCRP/IAPSO Work. Group 136. 2011. On the role of the Agulhas system in ocean circulation and climate. *Nature* 472:429–36

Bell DB, Jung SJA, Kroon D, Hodell DA, Lourens LJ, Raymo ME. 2015. Atlantic deep-water response to the early Pliocene shoaling of the Central American Seaway. *Sci. Rep.* 5:12252

Blanke B, Arhan M, Speich S. 2006. Salinity changes along the upper limb of the Atlantic thermohaline circulation. *Geophys. Res. Lett.* 33:L06609

Boccaletti G, Ferrari R, Adcroft A, Ferreira D, Marshall J. 2005. The vertical structure of ocean heat transport. *Geophys. Res. Lett.* 32:L10603

Böhm E, Lippold J, Gutjahr M, Frank M, Blaser P, et al. 2015. Strong and deep Atlantic meridional overturning circulation during the last glacial cycle. *Nature* 517:73–76

Borrelli C, Cramer BS, Katz ME. 2014. Bipolar Atlantic deepwater circulation in the middle-late Eocene: effects of Southern Ocean gateway openings. *Paleoceanography* 29:308–27

Boyle EA, Keigwin LD. 1985. Comparison of Atlantic and Pacific paleochemical records for the last 215,000 years: changes in deep ocean circulation and chemical inventories. *Earth Planet. Sci. Lett.* 76:135–50

Boyle EA, Keigwin LD. 1987. North Atlantic thermohaline circulation during the past 20,000 years linked to high-latitude surface temperature. *Nature* 330:35–40

Boyle PR, Romans BW, Tucholke BE, Norris RD, Swift SA, Sexton PF. 2017. Cenozoic North Atlantic deep circulation history recorded in contourite drifts, offshore Newfoundland, Canada. *Mar. Geol.* 385:185–203

Brass GW, Southam JR, Peterson WH. 1982. Warm saline bottom water in the ancient ocean. *Nature* 296:620–23

Broecker WS. 1991. The great ocean conveyor. *Oceanography* 4:79–89

Broecker WS, Peteet DM, Rind D. 1985. Does the ocean-atmosphere system have more than one stable mode of operation? *Nature* 315:21–26

Bryan F. 1986. High-latitude salinity effects and interhemispheric thermohaline circulations. *Nature* 323:301–4

Buckley MW, Marshall J. 2016. Observations, inferences, and mechanisms of the Atlantic meridional overturning circulation: a review. *Rev. Geophys.* 54:5–63

Burckel P, Waelbroeck C, Gherardi JM, Pichat S, Arz H, et al. 2015. Atlantic Ocean circulation changes preceded millennial tropical South America rainfall events during the last glacial. *Geophys. Res. Lett.* 42:411–18

Burls NJ, Fedorov AV, Sigman DM, Jaccard SL, Tiedemann R, Haug GH. 2017. Active Pacific meridional overturning circulation (PMOC) during the warm Pliocene. *Sci. Adv.* 3:e1700156

Burton KW, Ling HF, O'Nions RK. 1997. Closure of the Central American isthmus and its effect on deep-water formation in the North Atlantic. *Nature* 386:382–85

Busecke J, Abernathey RP, Gordon AL. 2017. Lateral eddy mixing in the subtropical salinity maxima of the global ocean. *J. Phys. Oceanogr.* 47:737–54

Cessi P, Jones CS. 2017. Warm-route versus cold-route interbasin exchange in the meridional overturning circulation. *J. Phys. Oceanogr.* 47:1981–97

Chen JL, Wilson CR, Tapley BD. 2006. Satellite gravity measurements confirm accelerated melting of Greenland ice sheet. *Science* 313:1958–60
Coxall HK, Huck CE, Huber M, Lear CH, Legarda-Lisarri A, et al. 2018. Export of nutrient rich Northern Component Water preceded early Oligocene Antarctic glaciation. *Nat. Geosci.* 11:190–96
Craig PM, Ferreira D, Methven J. 2017. The contrast between Atlantic and Pacific surface water fluxes. *Tellus A* 69:1330454
Cramer BS, Toggweiler JR, Wright JD, Katz ME, Miller GH. 2009. Ocean overturning since the Late Cretaceous: inferences from a new benthic foraminiferal isotope compilation. *Paleoceanography* 24:PA4216
Curry WB, Marchitto TM, McManus JF, Oppo DW, Laarkamp KL. 1999. Millennial-scale changes in ventilation of the thermocline, intermediate, and deep waters of the glacial North Atlantic. In *Mechanisms of Global Climate Change at Millennial Time Scales*, ed. PU Clark, RS Webb, LD Keigwin, pp. 59–76. Geophys. Monogr. Ser. 112. Washington, DC: Am. Geophys. U.
Curry WB, Oppo DW. 2005. Glacial water mass geometry and the distribution of $\delta^{13}C$ of CO_2 in the western Atlantic Ocean. *Paleoceanography* 24:PA1017
Czaja A. 2009. Atmospheric control on the thermohaline circulation. *J. Phys. Oceanogr.* 39:234–47
de Boer AM, Gnanadesikan A, Edwards NR, Watson AJ. 2010. Meridional density gradients do not control the Atlantic overturning circulation. *J. Phys. Oceanogr.* 40:368–80
de Boer AM, Nof D. 2004. The Bering Strait's grip on the northern hemisphere climate. *Deep-Sea Res. I* 51:1347–66
de Boer AM, Sigman D, Toggweiler JR, Russell JL. 2007. Effect of global ocean temperature change on deep ocean ventilation. *Paleoceanography* 22:PA2210
de Boer AM, Toggweiler JR, Sigman DM. 2008. Atlantic dominance of the meridional overturning circulation. *J. Phys. Oceanogr.* 38:435–50
de Vries P, Weber SL. 2005. The Atlantic freshwater budget as a diagnostic for the existence of a stable shut down of the meridional overturning circulation. *Geophys. Res. Lett.* 32:L09606
Dee D, Uppala S, Simmons A, Berrisford P, Poli P, et al. 2011. The ERA-Interim reanalysis: configuration and performance of the data assimilation system. *Q. J. R. Meteorol. Soc.* 137:553–97
den Toom M, Dijkstra HA, Cimatoribus AA, Drijfhout SS. 2012. Effect of atmospheric feedbacks on the stability of the Atlantic meridional overturning circulation. *J. Clim.* 25:4081–96
Dijkstra HA. 2007. Characterization of the multiple equilibria regime in a global ocean model. *Tellus A* 59:695–705
Donners J, Drijfhout SS. 2004. The Lagrangian view of South Atlantic interocean exchange in a global ocean model compared with inverse model results. *J. Clim.* 34:1019–35
Duplessy JC, Shackleton NJ, Fairbanks RG, Labeyrie L, Oppo D, Kallel N. 1988. Deepwater source variations during the last climatic cycle and their impact on global deepwater circulation. *Paleoceanography* 3:343–60
Durack PJ, Wijffels SE, Matear R. 2012. Ocean salinities reveal strong global water cycle intensification during 1950 to 2000. *Science* 336:455–58
Eichelberger SJ, Hartmann DL. 2007. Zonal jet structure and the leading mode of variability. *J. Clim.* 20:5149–63
Eldevik T, Risebrobakken B, Bjune AE, Andersson C, Birks HJB, et al. 2014. A brief history of climate—the northern seas from the Last Glacial Maximum to global warming. *Quat. Sci. Rev.* 106:225–46
Emile-Geay J, Cane MA, Naik N, Clement AC, van Geen A. 2003. Warren revisited: atmospheric freshwater fluxes and "Why is no deep water formed in the North Pacific." *J. Geophys. Res.* 108:3178
Ferrari R, Ferreira D. 2011. What processes drive the ocean heat transport? *Ocean Model.* 38:171–86
Ferreira D, Marshall J, Campin JM. 2010. Localization of deep water formation: role of atmospheric moisture transport and geometrical constraints on ocean circulation. *J. Clim.* 23:1456–76
Forget G, Campin JM, Heimbach P, Hill C, Ponte R, Wunsch C. 2015. ECCO version 4: an integrated framework for nonlinear inverse modeling and global ocean state estimation. *Geosci. Model Dev.* 8:3653–743
Frankignoul C. 1985. Sea surface temperature anomalies, planetary waves, and air-sea feedback in mid latitudes. *Rev. Geophys.* 23:357–90

Freeman E, Skinner LC, Tisserand A, Dokken T, Timmermann A, et al. 2015. An Atlantic-Pacific ventilation seesaw across the last deglaciation. *Earth Planet. Sci. Lett.* 424:237–44
Galaasen EV, Ninnemann US, Irval N, Kleiven HKF, Rosenthal Y, et al. 2014. Rapid reductions in North Atlantic deep water during the peak of the last interglacial period. *Nature* 343:1129–32
Garzoli SL, Baringera MO, Donga S, Pereza RC, Yaoa Q. 2013. South Atlantic meridional fluxes. *Deep-Sea Res. I* 71:21–32
Gebbie J, Huybers P. 2012. The mean age of ocean waters inferred from radiocarbon observations: sensitivity to surface sources and accounting for mixing histories. *J. Phys. Oceanogr.* 42:291–305
Gherardi JM, Labeyrie L, Nave S, Francois R, McManus JF, Cortijo E. 2009. Glacial-interglacial circulation changes inferred from $^{231}Pa/^{230}Th$ sedimentary records in the North Atlantic region. *Paleoceanography* 24:PA2204
Gnanadesikan A. 1999. A simple predictive model for the structure of the oceanic pycnocline. *Science* 283:2077–79
Gordon AL. 1986. Interocean exchange of thermocline water. *J. Geophys. Res.* 91:5037–46
Gregory JM, Dixon KW, Stouffer RJ, Weaver AJ, Driesschaert E, et al. 2005. A model intercomparison of changes in the Atlantic thermohaline circulation in response to increasing atmospheric CO_2 concentration. *Geophys. Res. Lett.* 32:L12703
Guihou A, Pichat S, Govin A, Nave S, Michel E, et al. 2011. Enhanced Atlantic meridional overturning circulation supports the Last Glacial Inception. *Quat. Sci. Rev.* 30:1576–82
Held IM, Soden BJ. 2006. Robust responses of the hydrological cycle to global warming. *J. Clim.* 19:5686–99
Henry LG, McManus JF, Curry WB, Roberts NL, Piotrowski AM, Keigwin LD. 2016. North Atlantic ocean circulation and abrupt climate change during the last glaciation. *Science* 353:470–74
Herold N, Huber M, Müller RD, Seton M. 2012. Modeling the Miocene climatic optimum: ocean circulation. *Paleoceanography* 27:PA1209
Hohbein MW, Sexton PF, Cartwright JA. 2012. Onset of North Atlantic deep water production coincident with inception of the Cenozoic global cooling trend. *Geology* 40:255–58
Hu AG, Meehl A, Han W, Abe-Ouchi A, Morrill C, et al. 2012. The Pacific-Atlantic seesaw and the Bering Strait. *Geophys. Res. Lett.* 39:L03702
Huisman SE, Dijkstra HA, von der Heydt A, de Ruijter WPM. 2012. Does net *E-P* set a preference for North Atlantic sinking? *J. Phys. Oceanogr.* 42:1781–92
Jackson LC, Smith RS, Wood RA. 2017. Ocean and atmosphere feedbacks affecting AMOC hysteresis in a GCM. *Clim. Dyn.* 49:173–91
Jia Y, Coward AC, de Cuevas BA, Webb DJ, Drijfhout S. 2007. A model analysis of the behavior of the Mediterranean Water in the North Atlantic. *J. Phys. Oceanogr.* 34:764–86
Johnson HL, Marshall DP, Sproson DAJ. 2007. Reconciling theories of a mechanically driven meridional overturning circulation with thermohaline forcing and multiple equilibria. *Clim. Dyn.* 29:821–36
Jones CS, Cessi P. 2016. Interbasin transport of the meridional overturning circulation. *J. Phys. Oceanogr.* 46:1157–69
Keigwin LD. 1987. North Pacific deep water formation during the latest glaciation. *Nature* 330:362–64
Keigwin LD, Swift SA. 2017. Carbon isotope evidence for a northern source of deep water in the glacial western North Atlantic. *PNAS* 114:2831–35
Knudson KP, Ravelo AC. 2015. North Pacific Intermediate Water circulation enhanced by the closure of the Bering Strait. *Paleoceanography* 20:1287–304
Kuhlbrodt T, Griesel A, Montoy M, Levermann A, Hofmann M, Rahmstorf S. 2007. On the driving processes of the Atlantic meridional overturning circulation. *Rev. Geophys.* 45:RG2001
Kwiek PB, Ravelo AC. 1999. Pacific Ocean intermediate and deep water circulation during the Pliocene. *Palaeogeogr. Palaeoclimatol. Palaeoecol.* 154:191–217
Laurian A, Drijfhout SS. 2011. Response of the South Atlantic circulation to an abrupt collapse of the Atlantic meridional overturning circulation. *Clim. Dyn.* 37:521–30
Leduc G, Vidal L, Tachikawa K, Rostek F, Sonzogni C, et al. 2007. Moisture transport across Central America as a positive feedback on abrupt climatic changes. *Nature* 445:908–11
Levang S, Schmitt RW. 2015. Centennial changes of the global water cycle in CMIP5 models. *J. Clim.* 28:6489–502

Lippold J, Luo Y, Francois R, Allen SE, Gherardi J, et al. 2012. Strength and geometry of the glacial Atlantic meridional overturning circulation. *Nat. Geosci.* 5:813–16
Lohmann G. 2003. Atmospheric and oceanic freshwater transport during weak Atlantic overturning circulation. *Tellus A* 55:438–49
Lynch-Stieglitz J, Adkins JF, Curry WB, Dokken T, Hall IR, et al. 2007. Atlantic meridional overturning circulation during the Last Glacial Maximum. *Science* 316:66–69
Lynch-Stieglitz J, Fairbanks RG. 1994. Strength and geometry of the glacial Atlantic meridional overturning circulation. *Nature* 369:41–43
Marotzke J, Willebrand J. 1991. Multiple equilibria of the global thermohaline circulation. *J. Phys. Oceanogr.* 21:1372–85
Marshall J, Schott F. 1999. Open ocean deep convection observations, models and theory. *Rev. Geophys.* 37:1–64
Marshall J, Speer K. 2012. Closure of the meridional overturning circulation through Southern Ocean upwelling. *Nat. Geosci.* 5:171–80
McCave IN, Manighetti B, Beveridge NAS. 1995. Circulation in the glacial North Atlantic inferred from grain-size measurements. *Nature* 374:149–52
McManus JF, Francois R, Gherardi J, Keigwin LD, Brown-Leger S. 2004. Collapse and rapid resumption of Atlantic meridional circulation linked to deglacial climate changes. *Nature* 428:824–37
McManus JF, Oppo DW, Cullen JL. 1999. A 0.5 million year record of millennial-scale climate variability in the North Atlantic. *Nature* 283:971–75
McManus JF, Oppo DW, Keigwin LD, Cullen JL, Bond GG. 2002. Thermohaline circulation and prolonged interglacial warmth in the North Atlantic. *Quat. Res.* 58:17–21
Mecking JV, Drijfhout SS, Jackson LC, Graham T. 2016. Stable AMOC off state in an eddy-permitting coupled climate model. *Clim. Dyn.* 47:2455–70
Mikolajewicz U, Maier-Reimer E, Crowley TJ, Kim KY. 1993. Effect of Drake and Panamanian gateways on the circulation of an ocean model. *Paleoceanography* 8:409–26
Miller KG, Tucholke BE. 1983. Development of Cenozoic abyssal circulation south of the Greenland-Scotland Ridge. In *Structure and Development of the Greenland-Scotland Ridge*, ed. MHP Bott, S Saxov, M Talwani, J Thiede, pp. 549–89. NATO Conf. Ser. 8. New York: Plenum Press
Moiroud M, Pucéat E, Donnadieu Y, Bayon G, Guiraud M, et al. 2016. Evolution of neodymium isotopic signature of seawater during the Late Cretaceous: implications for intermediate and deep circulation. *Gondwana Res.* 36:503–22
Mokeddem Z, McManus JF, Oppo DW. 2014. Oceanographic dynamics and the end of the last interglacial in the subpolar North Atlantic. *PNAS* 111:11263–68
Molnar P, Boos WR, Battisti DS. 2010. Orographic controls on climate and paleoclimate of Asia: thermal and mechanical roles for the Tibetan Plateau. *Annu. Rev. Earth Planet. Sci.* 38:77–102
Murphy DP, Thomas DJ. 2013. The evolution of Late Cretaceous deep-ocean circulation in the Atlantic basins: neodymium isotope evidence from South Atlantic drill sites for tectonic controls. *Geochem. Geophys. Geosyst.* 14:5323–40
Nikurashin M, Vallis G. 2012. A theory of the interhemispheric meridional overturning circulation and associated stratification. *J. Phys. Oceanogr.* 42:1652–67
Nilsson J, Langen PL, Ferreira D, Marshall J. 2013. Ocean basin geometry and the salinification of the Atlantic Ocean. *J. Clim.* 26:6163–84
Nisancioglu KH, Raymo ME, Stone PH. 2003. Reorganization of Miocene deep water circulation in response to the shoaling of the Central American Seaway. *Paleoceanography* 18:1006
Okazaki Y, Timmermann A, Menviel L, Harada N, Abe-Ouchi A, et al. 2010. Deepwater formation in the North Pacific during the last glacial termination. *Science* 329:200–4
Okumura YM, Deser C, Hu A, Timmermann A, Xie S. 2009. North Pacific climate response to freshwater forcing in the Subarctic North Atlantic: oceanic and atmospheric pathways. *J. Clim.* 22:1424–45
Oppo DW, McManus JF, Cullen JL. 2003. Deepwater variability in the Holocene epoch. *Nature* 422:277–78
Pithan F, Mauritsen T. 2014. Arctic amplification dominated by temperature feedbacks in contemporary climate models. *Nature* 7:181–84

Ponte RM, Vinogradova NT. 2016. An assessment of basic processes controlling mean surface salinity over the global ocean. *Geophys. Res. Lett.* 43:7052–58

Rae JW, Sarnthein M, Foster GL, Ridgwell A, Grootes PM, Elliott T. 2014. Deep water formation in the North Pacific and deglacial CO_2 rise. *Paleoceanography* 29:645–67

Rahmstorf S. 1996. On the freshwater forcing and transport of the Atlantic thermohaline circulation. *Clim. Dyn.* 12:799–811

Rahmstorf S, Crucifix M, Ganapolski A, Goosse H, Kamenkovich I, et al. 2005. Thermohaline circulation hysteresis: a model intercomparison. *Geophys. Res. Lett.* 32:L23605

Raymo ME, Oppo DW, Flower B, Hodell D, McManus JF, et al. 2004. Stability of North Atlantic water masses in the face of pronounced natural climate variability. *Paleoceanography* 19:PA2008

Raymo ME, Ruddiman WF, Shackleton NJ, Oppo DW. 1990. Evolution of Atlantic-Pacific $\delta^{13}C$ gradients over the last 2.5 m.y. *Earth Planet. Sci. Lett.* 97:353–68

Reid JL. 1961. On the temperature, salinity, and density differences between the Atlantic and Pacific Oceans in the upper kilometre. *Deep-Sea Res.* 7:265–75

Reid JL. 1979. On the contribution of the Mediterranean Sea outflow to the Norwegian-Greenland Sea. *Deep-Sea Res.* 26A:1199–223

Rintoul SR. 1991. South Atlantic interbasin exchange. *J. Geophys. Res.* 96:2675–92

Robinson LF, Adkins JF, Keigwin LD, Southon J, Fernandez DP, et al. 2005. Radiocarbon variability in the Western North Atlantic during the last deglaciation. *Science* 310:1469–73

Rooth C. 1982. Hydrology and ocean circulation. *Prog. Oceanogr.* 11:131–49

Roquet F, Madec G, Brodeau L, Nycander J. 2015. Defining a simplified yet "realistic" equation of state for seawater. *J. Phys. Oceanogr.* 45:2564–79

Sandström JW. 1916. *Meteorologische Studien im Schwedischen Hochgebirge*. Göteborg, Swed.: Wettergren & Kerber

Sardeshmukh PD, Hoskins BJ. 1988. The generation of global rotational flow by steady idealized tropical divergence. *J. Atmos. Sci.* 45:1228–51

Scher HD, Martin EE. 2004. Circulation in the Southern Ocean during the Paleogene inferred from neodymium isotopes. *Earth Planet. Sci. Lett.* 228:391–405

Schmitt RW, Bogden PS, Dorman CE. 1989. Evaporation minus precipitation and density fluxes for the North Atlantic. *J. Phys. Oceanogr.* 19:1208–21

Schmittner A, Silva TAM, Fraedrich K, Kirk E, Lunkeit F. 2012. Effects of mountains and ice sheets on global ocean circulation. *J. Clim.* 24:2814–29

Sgubin G, Swingedouw D, Drijfhout S, Mary Y, Bennabi A. 2017. Abrupt cooling over the North Atlantic in modern climate models. *Nat. Commun.* 8. **https://doi.org/10.1038/ncomms14375**

Sigman DM, Jaccard SL, Haugh GH. 2004. Polar ocean stratification in a cold climate. *Nature* 428:59–63

Sijp WP, England MH. 2009. Southern Hemisphere westerly wind control over the ocean's thermohaline circulation. *J. Clim.* 22:1277–86

Sinha B, Blaker AT, Hirshi JJM, Bonham S, Brand M, et al. 2012. Mountain ranges favor vigorous Atlantic meridional overturning. *Geophys. Res. Lett.* 39:L02705

Speich S, Blanke B, Madec G. 2001. Warm and cold water routes of an O.G.C.M. thermohaline conveyor belt. *Geophys. Res. Lett.* 28:311–14

Stommel H. 1948. The westward intensification of the wind-driven ocean currents. *Trans. Am. Geophys. Union* 29:202–6

Stommel H. 1961. Thermohaline convection with two stable regimes of flow. *Tellus A* 13:224–30

Stouffer RJ, Yin J, Gregory J, Dixon K, Spelman M, et al. 2006. Investigating the causes of the response of the thermohaline circulation to past and future climate changes. *J. Clim.* 19:1365–87

Straneo F. 2006. On the connection between dense water formation, overturning and poleward heat transport in a convective basin. *J. Phys. Oceanogr.* 36:1822–40

Studer AS, Martínez-Garcia A, Jaccard SL, Girault FE, Sigman DM, Haug GH. 2012. Enhanced stratification and seasonality in the Subarctic Pacific upon Northern Hemisphere glaciation—new evidence from diatom-bound nitrogen isotopes, alkenones and archaeal tetraethers. *Earth Planet. Sci. Lett.* 351–52:84–94

Sverdrup HU. 1947. Wind-driven current in a baroclinic ocean; with application to the equatorial currents of the Eastern Pacific. *PNAS* 33:318–26
Talley LD. 2003. Shallow, intermediate, and deep overturning components of the global heat budget. *J. Phys. Oceanogr.* 33:530–60
Talley LD. 2013. Closure of the global overturning circulation through the Indian, Pacific, and Southern Oceans: schematics and transports. *Oceanography* 26:80–97
Thiede J. 1979. History of the North Atlantic Ocean: evolution of an asymmetric zonal paleo-environment in a latitudinal ocean basin. In *Deep Drilling Results in the Atlantic Ocean: Continental Margins and Paleoenvironment*, ed. M Talwani, W Hay, WBF Ryan, pp. 275–96. Washington, DC: Am. Geophys. U.
Thomas DJ, Korty R, Huber M, Schubert JA, Haines B. 2014. Nd isotopic structure of the Pacific Ocean 70–30 Ma and numerical evidence for vigorous ocean circulation and ocean heat transport in a greenhouse world. *Paleoceanography* 29:454–69
Thomas DJ, Via RK. 2007. Neogene evolution of Atlantic thermohaline circulation: perspective from Walvis Ridge, southeastern Atlantic Ocean. *Paleoceanography* 22:PA2212
Thompson AJ, Stewart AL, Bischoff T. 2016. A multibasin residual-mean model for the global overturning circulation. *J. Phys. Oceanogr.* 46:2583–604
Thornalley DJ, Blaschek M, Davies FJ, Praetorius S, Oppo DW, et al. 2013. Long-term variations in Iceland-Scotland overflow strength during the Holocene. *Clim. Past* 9:2073–84
Thorpe RB, Gregory J, Johns T, Wood R, Mitchell J. 2001. Mechanisms determining the Atlantic thermohaline circulation response to greenhouse gas forcing in a nonflux-adjusted coupled climate model. *J. Clim.* 14:3102–16
Vellinga M, Wood R. 2002. Global climatic impacts of a collapse of the Atlantic thermohaline circulation. *Clim. Change* 54:251–67
Via RK, Thomas DJ. 2006. Evolution of Atlantic thermohaline circulation: early Oligocene onset of deep-water production in the North Atlantic. *Geology* 34:441–44
Voigt S, Jung C, Friedrich O, Frank M, Teschner C, Hoffmann J. 2013. Tectonically restricted deep-ocean circulation at the end of the Cretaceous greenhouse. *Earth Planet. Sci. Lett.* 369–70:169–77
von der Heydt A, Dijkstra HA. 2006. Effect of ocean gateways on the global ocean circulation in the late Oligocene and early Miocene. *Paleoceanography* 21:PA1011
Vörösmarty CJ, Fekete BM, Meybeck M, Lammers RB. 2000. Geomorphometric attributes of the global system of rivers at 30-minute spatial resolution. *J. Hydrol.* 237:17–39
Warren BA. 1983. Why is no deep water formed in the North Pacific? *J. Mar. Res.* 41:327–47
Weaver AJ, Bitz CM, Fanning AF, Holland MM. 1999. Thermohaline circulation: high-latitude phenomena and the difference between the Pacific and the Atlantic. *Annu. Rev. Earth Planet. Sci.* 27:231–85
Welander P. 1986. Thermohaline effects in the ocean circulation and related simple models. In *Large-Scale Transport Processes in Oceans and Atmosphere*, ed. J Willebrand, DLT Anderson, pp. 163–200. NATO ASI Ser. 190. Dordrecht, Neth.: Springer
Wills RC, Schneider T. 2015. Stationary eddies and the zonal asymmetry of net precipitation and ocean freshwater forcing. *J. Clim.* 28:5115–33
Wolfe CL, Cessi P. 2010. What sets the strength of the mid-depth stratification and overturning circulation in eddying ocean models? *J. Phys. Oceanogr.* 40:1520–38
Woodruff F, Savin SM. 1989. Miocene deepwater oceanography. *Paleoceanography* 4:87–140
Wright A, Miller KG. 1993. Southern Ocean influences on late Eocene to Miocene deepwater circulation. *Antarct. Res. Ser.* 60:1–25
Wunsch C, Heimbach P. 2013. Two decades of the Atlantic meridional overturning circulation: anatomy, variations, extremes, prediction, and overcoming its limitations. *J. Clim.* 26:7167–86
Yang S, Galbraith E, Palter J. 2014. Coupled climate impacts of the Drake Passage and the Panama Seaway. *Clim. Dyn.* 43:37
Yin J, Stouffer R. 2007. Comparison of the stability of the Atlantic thermohaline circulation in two coupled atmosphere-ocean general circulation models. *J. Clim.* 20:4293–315
Zachos JC, Pagani M, Sloan LC, Thomas E, Billups K. 2001. Trends, rhythms, and aberrations in global climate 65 Ma to present. *Science* 292:686–93

Zaucker F, Stocker TF, Broecker WS. 1994. Atmospheric freshwater fluxes and their effect on the global thermohaline circulation. *J. Geophys. Res.* 99:12443–57

Zika JD, Skliris N, Nurser AJG, Josey SA, Mudrykd L, Laliberté F. 2015. Maintenance and broadening of the ocean's salinity distribution by the water cycle. *J. Clim.* 28:9550–60

Zweng MM, Reagan JR, Antonov JI, Locarnini RA, Mishonov AV, et al. 2013. *World Ocean Atlas 2013*, Vol. 2: *Salinity*, ed. S Levitus, A. Mishonov. NOAA Atlas NESDIS 74. Silver Spring, MD: Natl. Ocean. Data Cent.

Annual Review
of Earth and
Planetary Sciences
Volume 46, 2018

Contents

Errata

An online log of corrections to *Annual Review of Earth and Planetary Sciences* articles may be found at http://www.annualreviews.org/errata/earth